

Optical Recording Reveals Novel Properties of GSK1016790A-Induced TRPV4 Channel Activity in Primary Human Endothelial Cells

Michelle N. Sullivan, Michael Francis, Natalie L. Pitts, Mark S. Taylor, and

Scott Earley

Vascular Physiology Research Group
Department of Biomedical Sciences
Colorado State University
Fort Collins, CO 80523, USA
(M.N.S., N.L.P., S.E.)

Department of Biology
Colorado State University
Fort Collins, CO 80523, USA
(N.L.P.)

Department of Physiology
University of South Alabama College of Medicine,
Mobile, AL 36688, USA
(M.F., M.S.T.)

Corresponding Author

Scott Earley, Ph.D.; Department of Biomedical Sciences, Colorado State University,
Fort Collins, CO 80523-1680, USA. Phone: (970) 491-2062; Fax: (970) 491-7569;
Email: Scott.Earley@colostate.edu.

Number of text pages: 34

Number of tables: 1

Number of figures: 5

Number of references: 48

Number of words – Abstract: 182

Number of words – Introduction: 685

Number of words – Discussion: 1,397

Non-standard abbreviations

4 α -PDD (4 α -phorbol 12,13-didecanoate), **AA** (arachadonic acid), **CPA** (cyclopiazonic acid), **eNOS** (endothelial nitric oxide synthase), **ER** (endoplasmic reticulum), **GSK1016790A** (N-((1S)-1-[[4-((2S)-2-[[2,4-dichlorophenyl)sulfonyl]amino]-3-hydroxypropanoyl)-1-piperazinyl]carbonyl]-3-methylbutyl)-1-benzothiophene-2-carboxamide), **IP₃R** (inositol trisphosphate receptor), **K_{Ca}** (Ca²⁺-activated potassium channels), **NO** (nitric oxide), **PLA₂** (phospholipase A₂), **SERCA** (sarcoplasmic/endoplasmic reticulum Ca²⁺ ATPase), **TIRFM** (total internal reflection fluorescence microscopy), **TRP** (transient receptor potential), **V** (vanilloid)

ABSTRACT

Critical functions of the vascular endothelium are regulated by changes in intracellular $[Ca^{2+}]$. Endothelial dysfunction is tightly associated with cardiovascular disease, and improved understanding of Ca^{2+} entry pathways in these cells will have a significant impact on human health. However, much remains unknown about Ca^{2+} influx channels in endothelial cells because they are difficult to study using conventional patch clamp electrophysiology. Here we describe a novel, highly efficient method for recording and analyzing Ca^{2+} -permeable channel activity in primary human endothelial cells using a unique combination of Total Internal Reflection Fluorescence Microscopy (TIRFM), custom software-based detection, and selective pharmacology. Our findings indicate that activity of the vanilloid (V) transient receptor potential (TRP) channel TRPV4 can be rapidly recorded and characterized at the single-channel level using this method, providing novel insight into channel function. Using this method, we show that although TRPV4 protein is evenly distributed throughout the plasma membrane, most channels are silent even during maximal stimulation with the potent TRPV4 agonist GSK1016790A. Furthermore, our findings indicate that GSK1016790A acts by recruiting previously inactive channels, rather than through increasing elevation of basal activity.

INTRODUCTION

Mechanisms controlling endothelial cell Ca^{2+} entry, removal, as well as dynamic release from and reuptake to intracellular stores play a central role in the regulation of vascular tone. For example, a rise in endothelial cell intracellular $[\text{Ca}^{2+}]$ generates nitric oxide (NO) by increasing the activity of endothelial nitric oxide synthase (eNOS) and elevates the activity of phospholipase A_2 (PLA_2), an enzyme that liberates arachidonic acid (AA) from the plasma membrane to provide substrate for the production of potent vasoactive factors (Vanhoutte, 2004). In addition, Ca^{2+} -activated K^+ (K_{Ca}) channels are directly stimulated by a rise in intracellular $[\text{Ca}^{2+}]$, leading to hyperpolarization of the membranes of both endothelial cells and electrically coupled vascular smooth muscle cells to elicit vasodilation (Kohler and Hoyer, 2007; Taylor et al., 2003; Whorton et al., 1984). As endothelial dysfunction is strongly correlated with common cardiovascular diseases, such as hypertension, stroke, and atherosclerosis, new technologies that advance our understanding of Ca^{2+} movement in these cells will have considerable clinical impact. Ca^{2+} influx via members of the transient receptor potential (TRP) superfamily of cation channels can cause endothelium-dependent vasodilation (Birnbaumer et al., 1996; Earley et al., 2009; Freichel et al., 2001; Kohler et al., 2006; Marrelli et al., 2007; Vriens et al., 2005), but, because ion channel activity is difficult to study in native endothelial cells, significant questions regarding the molecular identities and regulation of these channels remain unresolved.

Patch clamp electrophysiology is routinely used to study ion channel activity. This methodology yields invaluable insight into channel biophysics and pharmacology but also presents significant limitations. In the on-cell and inside-out patch clamp

configurations, channel activity can only be recorded from the small portion of the cell membrane present under the patch pipette. Furthermore, the on-cell configuration does not allow membrane voltage clamp. The traditional whole-cell configuration disrupts intracellular signaling pathways when the cell membrane is ruptured and cells are dialyzed with the patch pipette solution. In addition to these inherent limitations, further impediments are presented by the morphology of native endothelial cells. Obtaining and maintaining GΩ seals with these small, extremely flat cells is exceedingly difficult, and progress tends to be deliberate. Therefore, a goal of the current study was to develop a robust, efficient method that allows ion channel activity in endothelial cells to be studied under near-physiological conditions. Parker and colleagues described a method that can be adopted for this purpose using Total Internal Reflection Fluorescence Microscopy (TIRFM) to record the unitary activity of Ca²⁺-permeable ion channels expressed in *Xenopus* oocytes (Demuro and Parker, 2005). In TIRFM, a low energy evanescent field of illumination is created when incident light is angled such that all of the light is reflected away from the sample (Demuro and Parker, 2005). The wavelength of the evanescent field is equal to that of the incident light but only penetrates the cell surface to a depth of ~100 nm to illuminate fluorophores at or near the cell surface (Demuro and Parker, 2005). When cells are loaded with fluorescent Ca²⁺ indicator dyes, such as Fluo 4-AM, Ca²⁺ microdomains at the cell surface can be imaged (Demuro and Parker, 2005). This technique has significant throughput advantages over conventional patch clamp methods because it allows for simultaneous recording of all events that occur on the bottom surface of the cell (Demuro and Parker, 2006; Parker and Smith, 2010). In addition, the optical method is less invasive

compared to conventional voltage clamp methods and leaves the intracellular environment undisturbed.

For the current study, we adapted the TIRFM technique to record Ca^{2+} influx channel activity in primary human microvascular endothelial cells. In addition, we developed novel software (LC_Pro, an ImageJ plugin) for unbiased, automated detection and analysis of endothelial cell Ca^{2+} signals. Findings presented here demonstrate that the combination of TIRFM and Ca^{2+} signal autodetection with LC_Pro software is ideal for recording the activity of Ca^{2+} -permeable ion channels in endothelial cells. We report novel insight into regulation of TRPV4 channels by the small molecule agonist GSK1016790A gained from this method. These findings demonstrate that this methodology represents a significant improvement over the techniques currently used to study ion channel activity in primary cells.

MATERIALS AND METHODS

Cell Culture

Primary human microvascular endothelial cells from neonate dermis (Cell Systems CSC-2M1), passages 3-4, were used in these experiments. Cells were cultured in CSC Complete Medium (Cell Systems) supplemented with 10 mL Culture Boost (Cell Systems 4CB-500) and 1 mL Bac-Off® (Cell Systems). Cells were incubated at 37°C, 6% CO₂, media was changed every 2-3 days, and cells were subcultured when confluent using 0.05% trypsin-EDTA (Invitrogen). Initial resurrection of cells from stocks frozen in liquid nitrogen required coating the culture flask with Attachment Factor (Cell Systems) before addition of media and cells. Prior to experiments cells were trypsinized and plated (9×10^3 cells/mL) on 35 mm Mattek dishes (14 mm microwell, Fisher Scientific). Cells were incubated overnight at 37°C, 6% CO₂.

Total Internal Reflection Fluorescence Microscopy

TIRFM recordings (3 ms exposure time) were acquired using a through-the-lens TIRF system built around an inverted Olympus IX-70 microscope equipped with an Olympus PlanApo x60 oil-immersion lens (numeral aperature = 1.45) and an Andor iXON CCD camera. Cells were loaded with Fluo 4-AM (4 µM) for 20 minutes at 37°C, 6% CO₂ in the dark. Cells were washed with and imaged in a physiologic HEPES-buffered solution (in mM): 2.5 CaCl₂, 146 NaCl, 4.7 KCl, 0.6 MgSO₄, 0.15 NaHPO₄, 0.1 ascorbic acid, 8 glucose, 10 HEPES (pH 7.4). All experiments were performed at room

temperature (22-25°C). Each recording was 1000 frames and ~20-40 seconds in length.

LC_Pro Data Analysis

All data used in analyses were derived directly from the original TIRFM recordings. Recordings were processed using a custom algorithm implemented as a plugin (LC_Pro) for ImageJ software specifically designed to: 1) detect statistically significant fluorescent signals within background noise, 2) automatically define circular regions of interest (ROIs, 15 pixel diameter) centered at active sites containing statistically significant fluorescent signals, and 3) calculate mean fluorescence intensities within ROIs to determine specific event parameters. 8-bit gray scale TIFF image sequences are input into LC_Pro/ImageJ, initially specifying the ROI size (15 pixels) and the frame rate of the input video, and event statistics are generated as the final output, according to the program flow chart outlined in Francis et al., 2012 (Francis et al., 2012). Briefly, *Image Processing* was performed through a series of steps: normalization of 8-bit gray scale image stacks to 0.01% saturated pixels, generation of a background frame from a minimum intensity projection of the image sequence, subtraction of the background frame from the original image sequence, and subtraction of a mean intensity projection of the sequence from the background-subtracted image sequence. The resulting image sequence is then divided by the time-dependent standard deviation of the background-subtracted image sequence. The ImageJ Particle Analyzer java class was then used to assign best fit ellipses at the center of each event. During *Event Processing*, the mean intensity within each ROI (ellipse) was calculated

using a modified version of the multimeasure plugin for ImageJ. Events are defined as fluorescent signals that meet several criteria: 1) a spatial restriction of ≥ 12.56 pixels per frame, 2) a temporal restriction of ≥ 2 frames, and 3) signal that falls within $P < 0.01$ for Gaussian variation. The statistical rigor underlying these stringent criteria for event classification allow for substantially high signal-to-noise discrimination of fluorescent signals. *ROI Processing* follows, where location (x,y), spatial spread, amplitude, duration, attack time, and decay time were then calculated for each event. LC_Pro was customized for our study by the addition of a step in the program flow prior to the calculation of event duration (during *ROI Processing*) in which the left and right side differences between peak and baseline fluorescence (F) were calculated and expressed as ΔF . Duration is expressed as the time interval at 50% max peak fluorescence. Spatial spread is calculated as the area of the maximum best fit ellipse at 95% of the peak fluorescence of an event. The LC_Pro plugin for ImageJ can be downloaded from the ImageJ website: <http://imagej.nih.gov/ij/plugins/lc-pro/index.html>.

RNA Isolation and RT-PCR

Total RNA was extracted from endothelial cells (RNeasy Protect Mini Kit) and first-strand cDNA was synthesized using an Omniscript Reverse Transcriptase kit (both from QIAGEN, Valencia, CA). PCR was performed using primer sets specific for TRPV4 (Qiagen QT00077217), yielding a product of 149 bp. PCR products were resolved on 2% agarose gels. PCR reactions always included a template-free negative control. The PCR product was sequenced to confirm its identity.

Immunocytochemistry

Immunocytochemistry was used to confirm expression of TRPV4 in primary human microvascular endothelial cells. Cells were fixed with 4% formaldehyde for 10 minutes, permeabilized with methanol (-80°C), blocked with 2% bovine serum albumin (in phosphate buffered saline), and incubated with a primary rabbit monoclonal antibody specific to TRPV4 (1:250, Alomone Labs ACC-034) overnight at 4°C. Cells were washed and incubated with a fluorescent secondary antibody (goat anti-rabbit) conjugated with a Texas Red fluorophore (1:1000, Santa Cruz Biotechnology sc2780) for 2 hours at room temperature in the dark. Fluorescence images for immunocytochemistry were obtained using a FluoView 1000 laser-scanning confocal microscope (Olympus) and a $\times 60$, 1.4 numerical aperture oil immersion objective with the pinhole diameter set for 1 Airy Unit. Excitation of Texas Red was by illumination with the 543 nm line set at 74% transmission, and emission was collected using a variable band-pass filter set to 555–655 nm. Excitation of DAPI was by illumination with the 405 nm line set at 0.1% transmission, and emission was collected using a variable band-pass filter set 475-575 nm. All images were acquired at 1024 \times 1024 pixels at 4.0 μ s/pixel and were analyzed in ImageJ version 1.44b.

Statistics

All data are means \pm SE. Values of *n* refer to the number of cells for each experiment. Statistical tests used for each data set are as follows: One-way analysis of variance (ANOVA) was used to test for differences in whole-cell event frequency between treatments with Ca²⁺ free and CPA; where significant, individual groups were

compared using a Student-Newman-Keuls post hoc test (Figure 1b). Unpaired t-tests were used to determine whole-cell frequency differences with addition of 4 α -PDD (Figure 2e). Two-way ANOVA was used to test for differences in whole-cell frequency differences between treatments in both the ruthenium red and HC-067047 experiments as well as the detection method comparison experiments; where significant, individual groups were compared using a Student-Newman-Keuls post hoc test (Figure 2f, 2g, 5a). Paired t-tests were used to test for differences in the quantity of events and event sites before and after treatment with GSK1016790A (Figure 4b). For comparison of non-Gaussian distributed data, a Mann-Whitney rank sum test was used to determine significant differences (Table 1). A level of $P \leq 0.05$ was accepted as statistically significant for all experiments. Histograms were constructed and fit using OriginPro v8.5, and SigmaPlot v11.0 was used to make the figures. The concentration response curve (Figure 2d) was constructed by fitting data to a four parameter logistic equation (SigmaPlot v11.0).

RESULTS

Novel Subcellular Ca^{2+} Influx Events in Primary Human Microvascular Endothelial

Cells Localized, transient increases in fluorescence were observed at the surface of endothelial cells loaded with Fluo 4-AM and imaged using TIRFM (Movie 1, Figure 1a, Supplementary Figure 1). Recordings were analyzed using LC_Pro to automatically identify subcellular regions with statistically significant changes in surface fluorescence, and the location, amplitude ($\Delta F = \text{local current peak } F - \text{local current minimum } F$), spatial spread, duration, attack time (duration from 50% F to local peak F), and decay time (duration from local peak F to 50% F) of each event was determined. A noise threshold filter ($\Delta F \leq 0.1$) was established based on a common peak observed in event amplitude histograms under all recording conditions. Whole-cell event frequency (Hz) was calculated as total events per cell per second. Under basal conditions, events had a mean amplitude (ΔF) of 0.39 ± 0.01 , attack time of 0.88 ± 0.06 s, decay time of 0.99 ± 0.07 s, duration of 2.67 ± 0.13 s, whole-cell event frequency of 0.11 ± 0.02 Hz, and a spatial spread of $6.26 \pm 2.01 \mu\text{m}^2$ ($n = 125$). These Ca^{2+} signals are longer in duration compared to previously described Ca^{2+} events, such as Ca^{2+} sparks (Cheng et al., 1993), Ca^{2+} sparklets (2004), and Ca^{2+} pulsars (Ledoux et al., 2008) (Supplementary Table 1).

To determine if events recorded from endothelial cells using TIRFM result from Ca^{2+} influx from the extracellular solution or from Ca^{2+} release from intracellular stores, we disrupted Ca^{2+} release from the endoplasmic reticulum (ER) with the sarcoplasmic/endoplasmic reticulum Ca^{2+} ATPase (SERCA) pump inhibitor cyclopiazonic acid (CPA, 10 μM). To demonstrate the efficacy of CPA treatment, global

Ca^{2+} levels were recorded during administration. As expected, global Ca^{2+} levels initially rose upon addition of CPA, and fluorescence returned to basal levels within 15 minutes (Supplementary Figure 2). Recordings were obtained from cells pre-treated with CPA (15 min) to preclude the possibility of recording store-activated Ca^{2+} influx events. CPA had no effect on basal whole-cell event frequency (0.12 ± 0.04 Hz, $n = 40$ for control; 0.15 ± 0.05 Hz, $n = 31$ for CPA) (Figure 1b). In contrast, we observed that whole-cell event frequency was nearly abolished when Ca^{2+} was removed (no added Ca^{2+} , 3 mM ethylene glycol-bis(2-aminoethylether)-N,N,N',N'-tetraacetic acid (EGTA)) from the extracellular solution (0.12 ± 0.04 Hz, $n = 40$ for control; 0.01 ± 0.003 Hz, $n = 39$ for Ca^{2+} free) (Figure 1b). These findings indicate that the Ca^{2+} signals recorded using TIRFM represent Ca^{2+} influx from the extracellular solution.

Histograms for event amplitude, duration, attack time, decay time, and spatial spread were constructed (Figure 1c). Event amplitudes and durations were broadly distributed, suggesting that the recorded signals result from the activity of multiple types of Ca^{2+} influx channels that were active under these conditions.

Unitary TRPV4 Channel Activity Recorded using TIRFM TRPV4 was identified as a specific molecular target to further evaluate the utility of TIRFM for recording Ca^{2+} -permeable channel activity in endothelial cells. TRPV4 was selected because of its biophysical properties, tissue distribution, physiological significance, and available selective pharmacology. TRPV4 channels are slightly selective for Ca^{2+} ions ($P_{\text{Ca}^{2+}}/P_{\text{Na}^{+}} \sim 9:1$), are present in the endothelium of cerebral, mesenteric, as well as other arterial beds, and are involved in endothelium-dependent vasodilation (Brierley et al., 2008;

Marrelli et al., 2007; Voets et al., 2002; Yang et al., 2006). Furthermore, selective pharmacology, including a recently described TRPV4 inhibitor (HC-067047) (Everaerts et al., 2010) and TRPV4 activators (GSK1016790A and 4 α -PDD) (Thorneloe et al., 2008; Watanabe et al., 2002), is available.

To establish the presence of TRPV4 in the cells used for this study, reverse transcriptase-polymerase chain reaction (RT-PCR) was performed using total RNA prepared from primary human microvascular endothelial cells. A band was detected at the expected amplicon length of 149 bp, indicating that TRPV4 mRNA is present (Figure 2a). TRPV4 protein was detected by immunolabeling (Figure 2b), whereas very little fluorescence was present when the primary antibody was omitted (Figure 2c), indicating specificity of labeling. TRPV4 protein appears to be uniformly distributed throughout the cell (Figure 2b).

The effects of the potent TRPV4 agonist GSK1016790A (0.1 nM to 1 μ M) were recorded using TIRFM. GSK1016790A increased whole-cell event frequency in a concentration-dependent manner with a near maximal response at [GSK1016790A] \geq 100 nM ($n = 20$ -30 cells at each concentration) (Movie 2, Figure 2d). The EC₅₀ value determined from these data (26.9 nM) is within an order of magnitude of the reported EC₅₀ value (3 nM) determined using patch clamp electrophysiology for TRPV4 activation with GSK1016790A in a HEK 293 expression system (Thorneloe et al., 2008). GSK1016790A was used at a concentration of 100 nM in all subsequent experiments to achieve maximal stimulation. Cell death, indicated by an irreversible global increase in Ca²⁺, was observed in ~10% of cells exposed to GSK1016790A at this concentration. Data from cells that died during recording were excluded from analyses.

GSK1016790A-induced increases in whole-cell event frequency were abolished with removal of extracellular Ca^{2+} (0.07 ± 0.03 Hz ($n = 10$) for control, 0.01 ± 0.01 Hz ($n = 20$) for Ca^{2+} free + vehicle, and 0.002 ± 0.002 Hz ($n = 16$) for Ca^{2+} free + GSK1016790A (100 nM)), demonstrating that these events result from influx of extracellular Ca^{2+} . A second, structurally-distinct TRPV4 agonist, 4 α -PDD (10 μM), also increased whole-cell Ca^{2+} event frequency in primary endothelial cells (0.05 ± 0.02 Hz, $n = 13$ for control; 0.36 ± 0.10 Hz, $n = 21$ for 4 α -PDD) (Figure 2e). 11,12-epoxyeicosatrienoic acid (11,12-EET) is a potent vasodilator, activates TRPV4 channels (Watanabe et al., 2003) and is endogenously produced by vascular endothelial cells (Earley et al., 2003). 11,12-EET (3 μM) also increased the whole-cell frequency of Ca^{2+} events relative to vehicle (1% DMSO), (0.01 ± 0.01 Hz, $n = 18$ for vehicle; 0.05 ± 0.02 Hz, $n = 19$ for 11,12-EET) (Supplementary Figure 3). These findings demonstrate activation of TRPV4-mediated Ca^{2+} influx events in endothelial cells by an endogenously produced vasodilator.

The effects of the non-specific TRPV blocker ruthenium red (10 μM) and the selective TRPV4 blocker HC-067047 (500 nM) on baseline and GSK1016790A-stimulated (100 nM) Ca^{2+} events were examined. Cells were pre-treated with physiologic solution containing blocker (ruthenium red or HC-067047) or vehicle (distilled water for ruthenium red or DMSO for HC-067047) for 5 minutes at room temperature prior to experimentation. Neither blocker altered the basal Ca^{2+} influx event frequency (Figure 2f and g). In the absence of ruthenium red, GSK1016790A (100 nM) stimulated an increase in the whole-cell frequency of Ca^{2+} events recorded with TIRFM (0.05 ± 0.01 Hz, $n = 29$ vs. 0.38 ± 0.10 Hz, $n = 17$) (Figure 2F). A similar response to GSK1016790A (100 nM) was observed in the absence of HC-067047

treatment, (0.09 ± 0.04 Hz, $n = 26$ vs. 0.59 ± 0.11 Hz, $n = 19$) (Figure 2g). In contrast, GSK1016790A (100 nM) failed to stimulate an increase in event frequency in the presence of ruthenium red (0.11 ± 0.04 Hz, $n = 43$ vs. 0.15 ± 0.03 Hz, $n = 44$) or HC-067047 (0.05 ± 0.02 Hz, $n = 28$ vs. 0.18 ± 0.09 Hz, $n = 23$) (Figure 2f and g). Taken together, these findings indicate the presence of endogenous, functional TRPV4 channels in human microvascular endothelial cells and demonstrate that the activity of these channels can be recorded and analyzed using TIRFM and LC_Pro.

TRPV4-Mediated Ca^{2+} Influx Events are Distinct from Basal Events Ca^{2+} influx events stimulated by GSK1016790A (100 nM) were further characterized by histogram analysis of event amplitude, spatial spread, duration, attack time, and decay time (Figure 3b - d). Interestingly, a fit of event amplitudes displays quantal separation (i.e., $\Delta F = 0.12, 0.18, 0.23, 0.30$, etc.), suggesting that these signals represent the activity of an integral number of TRPV4 channels with a unitary ΔF value of ~ 0.06 ($n = 59$) (Figure 3b). Single TRPV4 channel activity ($\Delta F = 0.06$) is apparent in some tracings (Figure 3c) but could not be resolved from noise in most recordings. Spatial spread, duration, attack, and decay were all narrowly distributed around the respective means (Figure 3d), consistent with the activation of a single type of ion channel. The mean amplitude of GSK1016790A-induced events was smaller than that of control events and the mean duration, attack, and decay times were significantly shorter (Figure 3a, Table 1). Spatial spread did not differ between groups but tended to be smaller for GSK1016790A-induced Ca^{2+} influx events (Table 1).

TRPV4-mediated increases in whole-cell event frequency following agonist stimulation could be due to an elevation of the frequency of Ca^{2+} influx through basally active channels or could result from the recruitment of new event sites. To distinguish between these possibilities, endothelial cell Ca^{2+} events were recorded before and after stimulation with GSK1016790A (100 nM). The total number of events (4.78 ± 1.71 vs. 12.78 ± 3.33) and the number of event sites (4.22 ± 1.40 vs. 8.89 ± 1.86) per cell was increased following treatment with GSK1016790A (100 nM) ($n = 9$) (Figure 4). Masks of event sites detected by LC_Pro before and after agonist stimulation were constructed, color coded, and merged (Figure 4a). The sites active before (green) vs. after (red) agonist administration did not overlap. Of the 9 cells that were studied in this experiment, only two had a single site that was active both before and after administration of GSK1016790A. These findings indicate that basal and GSK1016790A-induced Ca^{2+} influx events are mediated by distinct populations of ion channels, and that quiescent TRPV4 channels are recruited by the agonist. Interestingly, although TRPV4 channels appear to be uniformly distributed throughout the endothelial cell plasma membrane (Figure 2b), we detected only a few sites of activity using TIRFM when a near-maximal concentration of GSK1016790A was administered (Figure 4a). These data suggest that much of the channel protein present in endothelial cells is either not present on the plasma membrane or is inactive under these conditions.

DISCUSSION

The goal of the current study was to develop an efficient method for investigating the activity of Ca^{2+} -permeable ion channels in primary endothelial cells. We find that: 1) novel, transient, subcellular Ca^{2+} influx events can be recorded from primary human endothelial cells and characterized using a combination of TIRFM and LC_Pro autodetection analysis, 2) the selective TRPV4 agonist GSK1016790A elicits concentration-dependent increases in the whole-cell frequency of Ca^{2+} influx events that are attenuated by TRPV4 antagonists and abolished in the absence of extracellular Ca^{2+} , 3) the peak amplitude distribution of GSK1016790A-induced Ca^{2+} influx events displays quantal separation, suggesting that single channel activity can be recorded, 4) GSK1016790A-induced Ca^{2+} influx events represent newly-recruited TRPV4 channels, rather than increased activity of previously established sites, and 5) much of the TRPV4 channels present in endothelial cells remain silent during maximal agonist stimulation. Together, these data demonstrate that basal and TRPV4 Ca^{2+} influx events can be distinguished and characterized using our combined TIRFM/LC_Pro approach. Moreover, our findings are consistent with the conclusion that GSK1016790A-activated Ca^{2+} influx events represent recruitable TRPV4 channel activity in primary endothelial cells. Importantly, these results establish that using TIRFM with selective pharmacology and LC_Pro autodetection to record Ca^{2+} -permeable ion channel activity in the endothelial cells improves experimental efficiency as well as sensitivity and provides spatial information not provided by conventional patch clamp techniques.

Changes in intracellular $[\text{Ca}^{2+}]$ mediate critical functions of the endothelium, including capillary permeability, changes in membrane potential, and production of

vasoactive substances. Because voltage clamp electrophysiology is difficult to efficiently apply to native endothelial cells due to their small size and flat morphology, much remains unknown about the Ca^{2+} influx pathways contributing to the regulation of these processes. The current findings demonstrate that TIRFM is a significant improvement over conventional patch clamp electrophysiology for studying Ca^{2+} influx channels in primary endothelial cells. Benefits of TIRFM compared to voltage clamp include higher throughput, the ability to record from cells in an unperturbed state, and the capability to simultaneously record the location and biophysical properties of multiple Ca^{2+} signals from each cell. In addition, the TIRFM approach provides spatial information that cannot be obtained using traditional patch clamp electrophysiology. The principle disadvantage of the TIRFM method is the lack of voltage clamp, but this can be compensated for by manipulating the ionic content of the extracellular solution. Additionally, the TIRFM technique detects only Ca^{2+} influx and does not measure outward currents or currents resulting from the movement of other ions, such as Na^+ or K^+ , that contribute to the total activity of nonselective cation channels. Despite these minor limitations, our findings clearly demonstrate the advantages of TIRFM for recording the activity of Ca^{2+} -permeable ion channel activity in endothelial cells. Confocal microscopy could also be used to study unitary Ca^{2+} influx events in endothelial cells. We selected TIRFM over confocal microscopy for the current study in order to be consistent with the method used in prior work studying Ca^{2+} influx channels (Demuro and Parker, 2005).

The findings of this study demonstrate that distinct types of Ca^{2+} influx events can be recorded from primary endothelial cells using a combination of TIRFM and

selective pharmacology. Prior reports suggest that endothelial cells express multiple Ca^{2+} influx channels, including several TRP channels (TRPC1, TRPC3, TRPC4, TRPV3, TRPV4, and TRPA1) (Chang et al., 1997; Earley et al., 2009; Earley et al., 2010; Freichel et al., 2001; Voets et al., 2002), the cyclic nucleotide-gated channel A1 (CNGA1) (Wu et al., 2000; Yao et al., 1999), and the ATP-sensitive purinergic ligand-gated receptor channel P2X4 (Yamamoto et al., 2000). Consistent with these observations, Ca^{2+} influx events recorded from unstimulated primary endothelial cells exhibit a broad distribution of event amplitude and duration, suggesting that these signals arise from more than one type of channel. This study provides the first evidence of spontaneous Ca^{2+} channel activity in primary human microvascular endothelial cells. The specific TIRFM properties of one channel, TRPV4, were characterized using selective pharmacological tools. Ca^{2+} signals stimulated by a TRPV4 agonist exhibited quantal separation in amplitude, were much shorter in duration (~8.5-fold), and tended to be larger in area compared with those recorded from unstimulated cells. These data establish a distinctive biophysical “TIRFM fingerprint” for TRPV4 channels in primary endothelial cells. Similar TRPV4 Ca^{2+} influx events were recently described in intact mouse mesenteric arteries (Sonkusare et al., 2012). Using a similar approach, other channels can be characterized and identified by their unique properties, enabling rapid identification of Ca^{2+} -permeable ion channels in endothelial and other types of cells. Thus, in addition to being a powerful research tool, the TIRFM/LC_Pro technique can be used in a clinical setting to study native endothelial cells under normal and pathophysiological conditions. For example, endothelial cells isolated from patients via peripheral artery biopsy (Colombo et al., 2002) could be examined by TIRFM/LC_Pro

for changes in endothelial cell Ca^{2+} channel activity associated with endothelial dysfunction and cardiovascular disease. The technique may be particularly useful for evaluating the mechanisms of action for drugs designed to improve endothelial function.

The selective agonist GSK1016790A has been extensively used to study the physiological role of TRPV4 channels (Gradilone et al., 2010; Jin et al., 2011; Mihara et al., 2011; Ryskamp et al., 2011; Thorneloe et al., 2008; Xu et al., 2009). However, little is currently known about how GSK1016790A stimulates TRPV4 channel activity. Application of the TIRFM technique revealed new insight into activation of TRPV4 activity by this agonist in primary endothelial cells. We show here for the first time that Ca^{2+} influx stimulated by GSK1016790A originates from newly-recruited, rather than from previously active, TRPV4 channels. These findings suggest that under the conditions used for this study, TRPV4 channels have a very low open probability. Consistent with this conclusion, neither ruthenium red nor the selective TRPV4 blocker HC-067047 diminished Ca^{2+} event frequency under basal conditions, suggesting that events recorded under basal conditions are very unlikely to be mediated by TRPV4 or any other TRPV channel. Interestingly, even maximal stimulation of TRPV4 channels with GSK1016790A produced only relatively modest increases in the whole cell frequency of Ca^{2+} influx events and event sites. These findings are consistent with those recently reported by Sonkusare et al. (Sonkusare et al., 2012), demonstrating that activation of as few as 3 TRPV4 channels per endothelial cell is sufficient to induce maximal dilation of mouse mesenteric arteries. In addition, the current findings also show that much of the TRPV4 channel protein present in primary endothelial cells is inactive during maximal agonist stimulation. The role of “silent” TRPV4 channels in

endothelial cells is unclear. It is possible that most of the TRPV4 protein present in primary endothelial cells is not expressed on the plasma membrane, and is either non-functional or contributes to cellular signaling in a manner that does not involve transport of ions across the plasma membrane. Non-conducting roles for other TRP channels (TRPM1, TRPM6, TRPM7, TRPM2, TRPP1, and TRPP2), hyperpolarization-activated cyclic nucleotide-gated (HCN) channels, as well as several K⁺ channels (Kv1.3, Kv10.1, and Kv11.1) have been reported (Duncan et al., 1998; Grimm et al., 2006; Huang, 2004; Pardo, 2004; Perraud et al., 2001; Runnels et al., 2001; Schlingmann et al., 2002; Zhong et al., 2004). These studies demonstrate contributions of non-conducting channels to numerous cellular processes including proliferation, mitogen activating protein (MAP) kinase signaling, tumor suppression, synaptic facilitation and channel expression (Duncan et al., 1998; Grimm et al., 2006; Huang, 2004; Pardo, 2004; Perraud et al., 2001; Runnels et al., 2001; Schlingmann et al., 2002; Zhong et al., 2004). It is also possible that conducting TRPV4 channels are present on intracellular membranes, such as the ER or Golgi bodies. Additional work is needed to determine the specific role of non-conducting TRPV4 channels in endothelial cells.

In summary, findings presented here demonstrate that TIRFM can be combined with selective pharmacological tools to establish characteristic properties of TRPV4 channels, suggesting that this approach can be used to study the activity of specific Ca²⁺-permeable ion channels. Using this method, we identified new information regarding the activation of TRPV4 by the small molecule agonist GSK1016790A. Furthermore, the findings of this study demonstrate that the novel combination of TIRFM and custom automatic ROI detection software is a significantly improved method

for recording and analyzing the activity of Ca^{2+} -permeable ion channels in primary endothelial cells. The approach described here may be effective for studying changes in endothelial cell Ca^{2+} channel activity during endothelial dysfunction associated with cardiovascular disease.

ACKNOWLEDGEMENTS

We thank Dr. Albert L. Gonzales for technical assistance and critical comments on the manuscript, Dr. Michael M. Tamkun for critical comments on the manuscript, and Dr. Gregory C. Amberg for technical advice.

AUTHORSHIP CONTRIBUTIONS

Participated in research design: Earley and Pitts.

Conducted experiments: Sullivan.

Contributed new reagents or analytic tools: Francis and Taylor.

Performed data analysis: Sullivan and Earley.

Wrote or contributed to writing/editing of manuscript: Earley and Sullivan.

REFERENCES

- (2004) [Microscopic mechanism of excitation-contraction coupling in cardiac myocytes]. *Sheng Li Ke Xue Jin Zhan* **35**(4): 294-298.
- Birnbaumer L, Zhu X, Jiang M, Boulay G, Peyton M, Vannier B, Brown D, Platano D, Sadeghi H, Stefani E and Birnbaumer M (1996) On the molecular basis and regulation of cellular capacitative calcium entry: roles for Trp proteins. *Proc Natl Acad Sci U S A* **93**(26): 15195-15202.
- Brierley SM, Page AJ, Hughes PA, Adam B, Liebrechts T, Cooper NJ, Holtmann G, Liedtke W and Blackshaw LA (2008) Selective role for TRPV4 ion channels in visceral sensory pathways. *Gastroenterology* **134**(7): 2059-2069.
- Chang AS, Chang SM, Garcia RL and Schilling WP (1997) Concomitant and hormonally regulated expression of trp genes in bovine aortic endothelial cells. *FEBS Lett* **415**(3): 335-340.
- Cheng H, Lederer WJ and Cannell MB (1993) Calcium sparks: elementary events underlying excitation-contraction coupling in heart muscle. *Science* **262**(5134): 740-744.
- Colombo PC, Ashton AW, Celaj S, Talreja A, Banchs JE, Dubois NB, Marinaccio M, Malla S, Lachmann J, Ware JA and Le Jemtel TH (2002) Biopsy coupled to quantitative immunofluorescence: a new method to study the human vascular endothelium. *J Appl Physiol* **92**(3): 1331-1338.
- Demuro A and Parker I (2005) "Optical patch-clamping": single-channel recording by imaging Ca²⁺ flux through individual muscle acetylcholine receptor channels. *J Gen Physiol* **126**(3): 179-192.
- Demuro A and Parker I (2006) Imaging single-channel calcium microdomains. *Cell Calcium* **40**(5-6): 413-422.
- Duncan LM, Deeds J, Hunter J, Shao J, Holmgren LM, Woolf EA, Tepper RI and Shyjan AW (1998) Down-regulation of the novel gene melastatin correlates with potential for melanoma metastasis. *Cancer Res* **58**(7): 1515-1520.
- Earley S, Gonzales AL and Crnich R (2009) Endothelium-dependent cerebral artery dilation mediated by TRPA1 and Ca²⁺-Activated K⁺ channels. *Circ Res* **104**(8): 987-994.
- Earley S, Gonzales AL and Garcia ZI (2010) A dietary agonist of transient receptor potential cation channel V3 elicits endothelium-dependent vasodilation. *Mol Pharmacol* **77**(4): 612-620.
- Earley S, Pastuszyn A and Walker BR (2003) Cytochrome p-450 epoxygenase products contribute to attenuated vasoconstriction after chronic hypoxia. *Am J Physiol Heart Circ Physiol* **285**(1): H127-136.
- Everaerts W, Zhen X, Ghosh D, Vriens J, Gevaert T, Gilbert JP, Hayward NJ, McNamara CR, Xue F, Moran MM, Strassmaier T, Uykai E, Owsianik G, Vennekens R, De Ridder D, Nilius B, Fanger CM and Voets T (2010) Inhibition of the cation channel TRPV4 improves bladder function in mice and rats with cyclophosphamide-induced cystitis. *Proc Natl Acad Sci U S A* **107**(44): 19084-19089.
- Francis M, Qian X, Charbel C, Ledoux J, Parker JC and Taylor MS (2012) Automated region of interest analysis of dynamic Ca²⁺ signals in image sequences. *Am J Physiol Cell Physiol*.
- Freichel M, Suh SH, Pfeifer A, Schweig U, Trost C, Weissgerber P, Biel M, Philipp S, Freise D, Droogmans G, Hofmann F, Flockerzi V and Nilius B (2001) Lack of an endothelial store-

- operated Ca²⁺ current impairs agonist-dependent vasorelaxation in TRP4^{-/-} mice. *Nat Cell Biol* **3**(2): 121-127.
- Gradilone SA, Masyuk TV, Huang BQ, Banales JM, Lehmann GL, Radtke BN, Stroope A, Masyuk AI, Splinter PL and LaRusso NF (2010) Activation of Trpv4 reduces the hyperproliferative phenotype of cystic cholangiocytes from an animal model of ARPKD. *Gastroenterology* **139**(1): 304-314 e302.
- Grimm DH, Karihaloo A, Cai Y, Somlo S, Cantley LG and Caplan MJ (2006) Polycystin-2 regulates proliferation and branching morphogenesis in kidney epithelial cells. *J Biol Chem* **281**(1): 137-144.
- Hellman B, Gylfe E, Grapengiesser E, Lund PE and Berts A (1992) Cytoplasmic Ca²⁺ oscillations in pancreatic beta-cells. *Biochim Biophys Acta* **1113**(3-4): 295-305.
- Huang CL (2004) The transient receptor potential superfamily of ion channels. *J Am Soc Nephrol* **15**(7): 1690-1699.
- Jin M, Wu Z, Chen L, Jaimes J, Collins D, Walters ET and O'Neil RG (2011) Determinants of TRPV4 activity following selective activation by small molecule agonist GSK1016790A. *PLoS One* **6**(2): e16713.
- Kohler R, Heyken WT, Heinau P, Schubert R, Si H, Kacik M, Busch C, Grgic I, Maier T and Hoyer J (2006) Evidence for a functional role of endothelial transient receptor potential V4 in shear stress-induced vasodilatation. *Arterioscler Thromb Vasc Biol* **26**(7): 1495-1502.
- Kohler R and Hoyer J (2007) The endothelium-derived hyperpolarizing factor: insights from genetic animal models. *Kidney Int* **72**(2): 145-150.
- Ledoux J, Taylor MS, Bonev AD, Hannah RM, Solodushko V, Shui B, Tallini Y, Kotlikoff MI and Nelson MT (2008) Functional architecture of inositol 1,4,5-trisphosphate signaling in restricted spaces of myoendothelial projections. *Proc Natl Acad Sci U S A* **105**(28): 9627-9632.
- Marrelli SP, O'Neil R G, Brown RC and Bryan RM, Jr. (2007) PLA2 and TRPV4 channels regulate endothelial calcium in cerebral arteries. *Am J Physiol Heart Circ Physiol* **292**(3): H1390-1397.
- Mihara H, Boudaka A, Sugiyama T, Moriyama Y and Tominaga M (2011) Transient receptor potential vanilloid 4 (TRPV4)-dependent calcium influx and ATP release in mouse oesophageal keratinocytes. *J Physiol* **589**(Pt 14): 3471-3482.
- Pardo LA (2004) Voltage-gated potassium channels in cell proliferation. *Physiology (Bethesda)* **19**: 285-292.
- Parker I and Smith IF (2010) Recording single-channel activity of inositol trisphosphate receptors in intact cells with a microscope, not a patch clamp. *J Gen Physiol* **136**(2): 119-127.
- Perraud AL, Fleig A, Dunn CA, Bagley LA, Launay P, Schmitz C, Stokes AJ, Zhu Q, Bessman MJ, Penner R, Kinet JP and Scharenberg AM (2001) ADP-ribose gating of the calcium-permeable LTRPC2 channel revealed by Nudix motif homology. *Nature* **411**(6837): 595-599.
- Runnels LW, Yue L and Clapham DE (2001) TRP-PLIK, a bifunctional protein with kinase and ion channel activities. *Science* **291**(5506): 1043-1047.
- Ryskamp DA, Witkovsky P, Barabas P, Huang W, Koehler C, Akimov NP, Lee SH, Chauhan S, Xing W, Renteria RC, Liedtke W and Krizaj D (2011) The polymodal ion channel

- transient receptor potential vanilloid 4 modulates calcium flux, spiking rate, and apoptosis of mouse retinal ganglion cells. *J Neurosci* **31**(19): 7089-7101.
- Schlingmann KP, Weber S, Peters M, Niemann Nejsum L, Vitzthum H, Klingel K, Kratz M, Haddad E, Ristoff E, Dinour D, Syrrou M, Nielsen S, Sassen M, Waldegger S, Seyberth HW and Konrad M (2002) Hypomagnesemia with secondary hypocalcemia is caused by mutations in TRPM6, a new member of the TRPM gene family. *Nat Genet* **31**(2): 166-170.
- Sonkusare SK, Bonev AD, Ledoux J, Liedtke W, Kotlikoff MI, Heppner TJ, Hill-Eubanks DC and Nelson MT (2012) Elementary Ca²⁺ signals through endothelial TRPV4 channels regulate vascular function. *Science* **336**(6081): 597-601.
- Taylor MS, Bonev AD, Gross TP, Eckman DM, Brayden JE, Bond CT, Adelman JP and Nelson MT (2003) Altered expression of small-conductance Ca²⁺-activated K⁺ (SK3) channels modulates arterial tone and blood pressure. *Circ Res* **93**(2): 124-131.
- Thorneloe KS, Sulpizio AC, Lin Z, Figueroa DJ, Clouse AK, McCafferty GP, Chendrimada TP, Lashinger ES, Gordon E, Evans L, Misajet BA, Demarini DJ, Nation JH, Casillas LN, Marquis RW, Votta BJ, Sheardown SA, Xu X, Brooks DP, Laping NJ and Westfall TD (2008) N-((1S)-1-([4-((2S)-2-[(2,4-dichlorophenyl)sulfonyl]amino)-3-hydroxypropyl)-1-piperazinyl]carbonyl)-3-methylbutyl)-1-benzothiophene-2-carboxamide (GSK1016790A), a novel and potent transient receptor potential vanilloid 4 channel agonist induces urinary bladder contraction and hyperactivity: Part I. *J Pharmacol Exp Ther* **326**(2): 432-442.
- Tsien RY, Rink TJ and Poenie M (1985) Measurement of cytosolic free Ca²⁺ in individual small cells using fluorescence microscopy with dual excitation wavelengths. *Cell Calcium* **6**(1-2): 145-157.
- Vanhoutte PM (2004) Endothelium-dependent hyperpolarizations: the history. *Pharmacol Res* **49**(6): 503-508.
- Voets T, Prenen J, Vriens J, Watanabe H, Janssens A, Wissenbach U, Boddling M, Droogmans G and Nilius B (2002) Molecular determinants of permeation through the cation channel TRPV4. *J Biol Chem* **277**(37): 33704-33710.
- Vriens J, Owsianik G, Fisslthaler B, Suzuki M, Janssens A, Voets T, Morisseau C, Hammock BD, Fleming I, Busse R and Nilius B (2005) Modulation of the Ca²⁺ permeable cation channel TRPV4 by cytochrome P450 epoxygenases in vascular endothelium. *Circ Res* **97**(9): 908-915.
- Watanabe H, Davis JB, Smart D, Jerman JC, Smith GD, Hayes P, Vriens J, Cairns W, Wissenbach U, Prenen J, Flockerzi V, Droogmans G, Benham CD and Nilius B (2002) Activation of TRPV4 channels (hVRL-2/mTRP12) by phorbol derivatives. *J Biol Chem* **277**(16): 13569-13577.
- Watanabe H, Vriens J, Prenen J, Droogmans G, Voets T and Nilius B (2003) Anandamide and arachidonic acid use epoxyeicosatrienoic acids to activate TRPV4 channels. *Nature* **424**(6947): 434-438.
- Wellman GC, Nathan DJ, Saundry CM, Perez G, Bonev AD, Penar PL, Tranmer BI and Nelson MT (2002) Ca²⁺ sparks and their function in human cerebral arteries. *Stroke* **33**(3): 802-808.
- Whorton AR, Willis CE, Kent RS and Young SL (1984) The role of calcium in the regulation of prostacyclin synthesis by porcine aortic endothelial cells. *Lipids* **19**(1): 17-24.

- Wu S, Moore TM, Brough GH, Whitt SR, Chinkers M, Li M and Stevens T (2000) Cyclic nucleotide-gated channels mediate membrane depolarization following activation of store-operated calcium entry in endothelial cells. *J Biol Chem* **275**(25): 18887-18896.
- Xu X, Gordon E, Lin Z, Lozinskaya IM, Chen Y and Thorneloe KS (2009) Functional TRPV4 channels and an absence of capsaicin-evoked currents in freshly-isolated, guinea-pig urothelial cells. *Channels (Austin)* **3**(3): 156-160.
- Yamamoto K, Korenaga R, Kamiya A, Qi Z, Sokabe M and Ando J (2000) P2X(4) receptors mediate ATP-induced calcium influx in human vascular endothelial cells. *Am J Physiol Heart Circ Physiol* **279**(1): H285-292.
- Yang XR, Lin MJ, McIntosh LS and Sham JS (2006) Functional expression of transient receptor potential melastatin- and vanilloid-related channels in pulmonary arterial and aortic smooth muscle. *Am J Physiol Lung Cell Mol Physiol* **290**(6): L1267-1276.
- Yao X, Leung PS, Kwan HY, Wong TP and Fong MW (1999) Rod-type cyclic nucleotide-gated cation channel is expressed in vascular endothelium and vascular smooth muscle cells. *Cardiovasc Res* **41**(1): 282-290.
- Zhong N, Beaumont V and Zucker RS (2004) Calcium influx through HCN channels does not contribute to cAMP-enhanced transmission. *J Neurophysiol* **92**(1): 644-647.

FOOTNOTES

Financial Support

This work was supported by the National Institute of Health [Grants R01HL091905 to SE, R01HL085887 to MST].

Parts of these data were presented in poster sessions at the Experimental Biology meeting in 2011 (Washington D.C.).

FIGURE LEGENDS

Figure 1. Novel Subcellular Ca^{2+} Influx Events in Primary Human Microvascular Endothelial Cells.

(a) Pseudocolor time lapse of a typical Ca^{2+} event recorded under control conditions; scale bar = 8 μm . (b) Mean data showing that depleting intracellular Ca^{2+} stores by pretreating with the SERCA pump inhibitor cyclopiazonic acid (CPA, 10 μM) had no effect on whole-cell (WC) event frequency, whereas removing extracellular Ca^{2+} diminished event frequency; $n = 40$ for control, $n = 31$ for CPA, $n = 39$ for Ca^{2+} free; $*P \leq 0.05$ vs. control. (c) Histograms of event amplitude, spatial spread, duration, attack time, and decay time. Event amplitudes and duration are randomly distributed, suggesting that multiple types of Ca^{2+} channels are active under basal conditions; $n = 125$ cells.

Figure 2, Unitary TRPV4 Channel Activity Recorded using TIRFM.

(a) RT-PCR for TRPV4 using total RNA from primary endothelial cells (EC) compared to a no DNA template control (NT); representative of 3 experiments. (b) Compressed z-stack images of immunolabeled TRPV4 (red) in primary endothelial cells vs. no primary antibody control (c). Nuclei are labeled with DAPI (blue); scale bar = 10 μm . Representative of 3 experiments. (d) Concentration response curve showing the effects of the selective TRPV4 agonist GSK1016790A on whole-cell (WC) Ca^{2+} event frequency. (e) Mean data showing that the TRPV4 agonist 4 α -PDD (10 μM) also increases the whole-cell (WC) frequency of Ca^{2+} influx events; $n = 13$ for control, $n = 21$ for 4 α -PDD; $*P \leq 0.05$ vs. control. Pretreatment with the non-specific TRPV blocker ruthenium red (10 μM) (f) or the selective TRPV4 inhibitor HC-067047 (500 nM) (g)

decreased the stimulation of Ca^{2+} event frequency in response to GSK1016790A (100 nM) but had no effect on baseline event frequency. For ruthenium red experiments, under baseline conditions $n = 29$ for control and $n = 43$ for ruthenium red, in the presence of GSK1016790A $n = 17$ for control and $n = 44$ for ruthenium red. For HC-067047 experiments, under baseline conditions $n = 26$ for control and $n = 28$ for HC-067047, in the presence of GSK1016790A- $n = 19$ for control and $n = 23$ for HC-067047; *NS* = No statistically significant differences detected; $*P \leq 0.05$ vs. control.

Figure 3. TRPV4-Mediated Ca^{2+} Influx Events are Distinct from Basal Events.

(a) Pseudocolor time lapse of a typical Ca^{2+} event recorded from a cell treated with GSK1016790A (100 nM); scale bar = 8 μm . (b) Histogram analysis of Ca^{2+} event amplitude in cells treated with GSK1016790A indicating quantal separation. These event levels can also be observed in a representative plot of fluorescence vs. time (c). (d) Histograms of spatial spread, duration, attack, and decay in cells treated with GSK1016790A.

Figure 4. GSK1016790A Increases Whole-Cell Event Frequency by Recruiting New Ca^{2+} Event Sites.

(a) (Top) TIRFM image of a typical primary endothelial cell. Ca^{2+} influx sites detected by LC_Pro for the indicated region are shown before (left) and after (middle) addition of GSK1016790A (100 nM). The merged pseudocolor image (right) shows events before addition of GSK1016790A in green and after in red. There is no overlap between the event sites. (b) Mean data showing the number of events (left) and the number of event

sites (right) per cell before and after addition of GSK1016790A (4.78 ± 1.71 events/cell before vs. 12.78 ± 3.33 events/cell after and 4.22 ± 1.40 sites/cell before vs. 8.89 ± 1.86 sites/cell after, $n = 9$ for each group); $*P \leq 0.05$ vs. control.

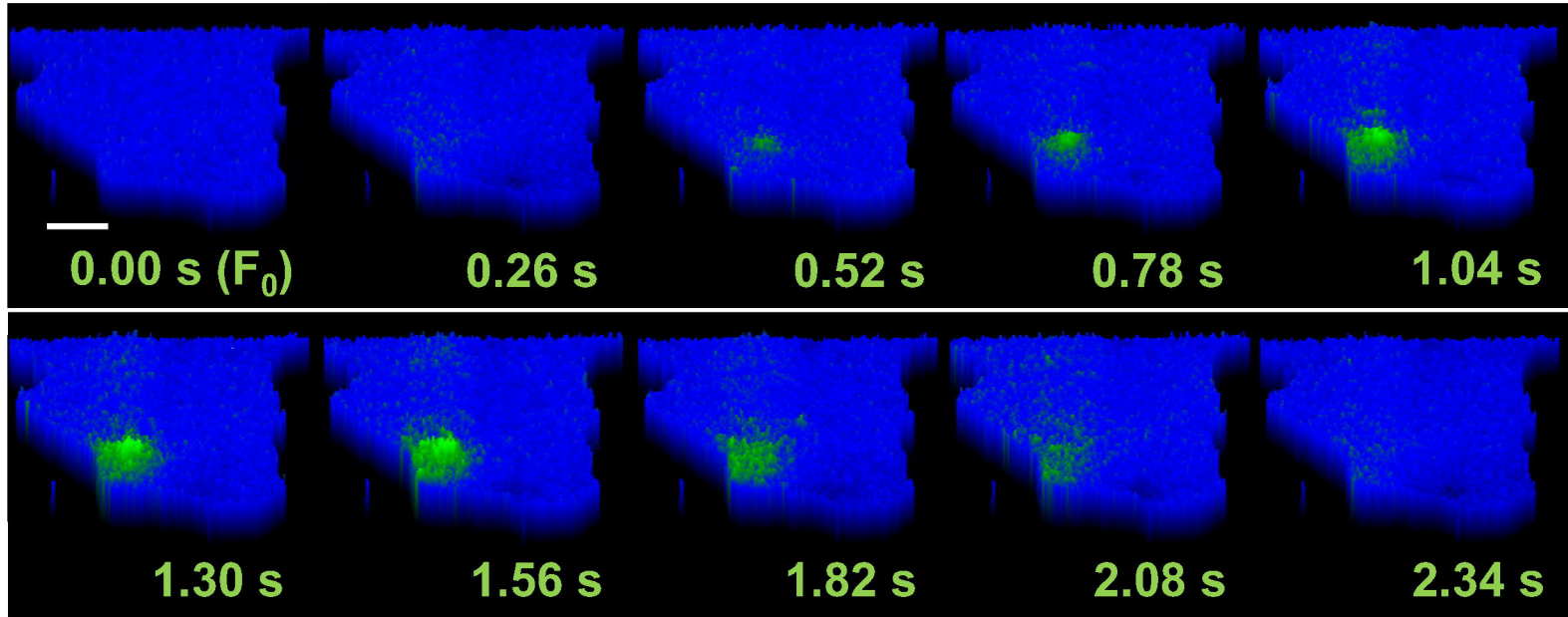
Table 1. Comparison of Basal Ca²⁺ Influx Events vs. GSK1016790A-Induced Events.

Amplitude, duration, attack time, decay time, spatial spread, and whole-cell (WC) frequency (mean ± SE) of Ca²⁺ influx events recorded from primary endothelial cells under basal condition (control) or following treatment with the selective TRPV4 agonist GSK1016790A (100 nM). *P ≤ 0.05 vs. control (Mann-Whitney rank sum test); *n* = 125 for control; *n* = 59 for GSK1016790A.

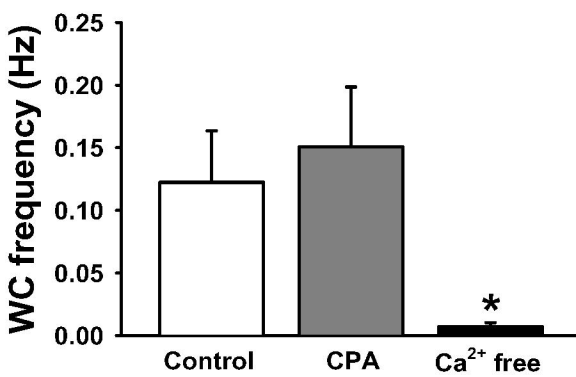
Parameter	Control	GSK1016790A
Amplitude (ΔF)	0.39 ± 0.01	0.22 ± 0.01*
Duration (s)	2.67 ± 0.13	0.52 ± 0.04*
Attack time (s)	0.88 ± 0.06	0.32 ± 0.02*
Decay time (s)	0.99 ± 0.07	0.37 ± 0.03*
Spatial spread (μm²)	6.26 ± 2.01	4.84 ± 0.82
WC frequency (Hz)	0.11 ± 0.02	0.48 ± 0.05*

Figure 1

a



b



c

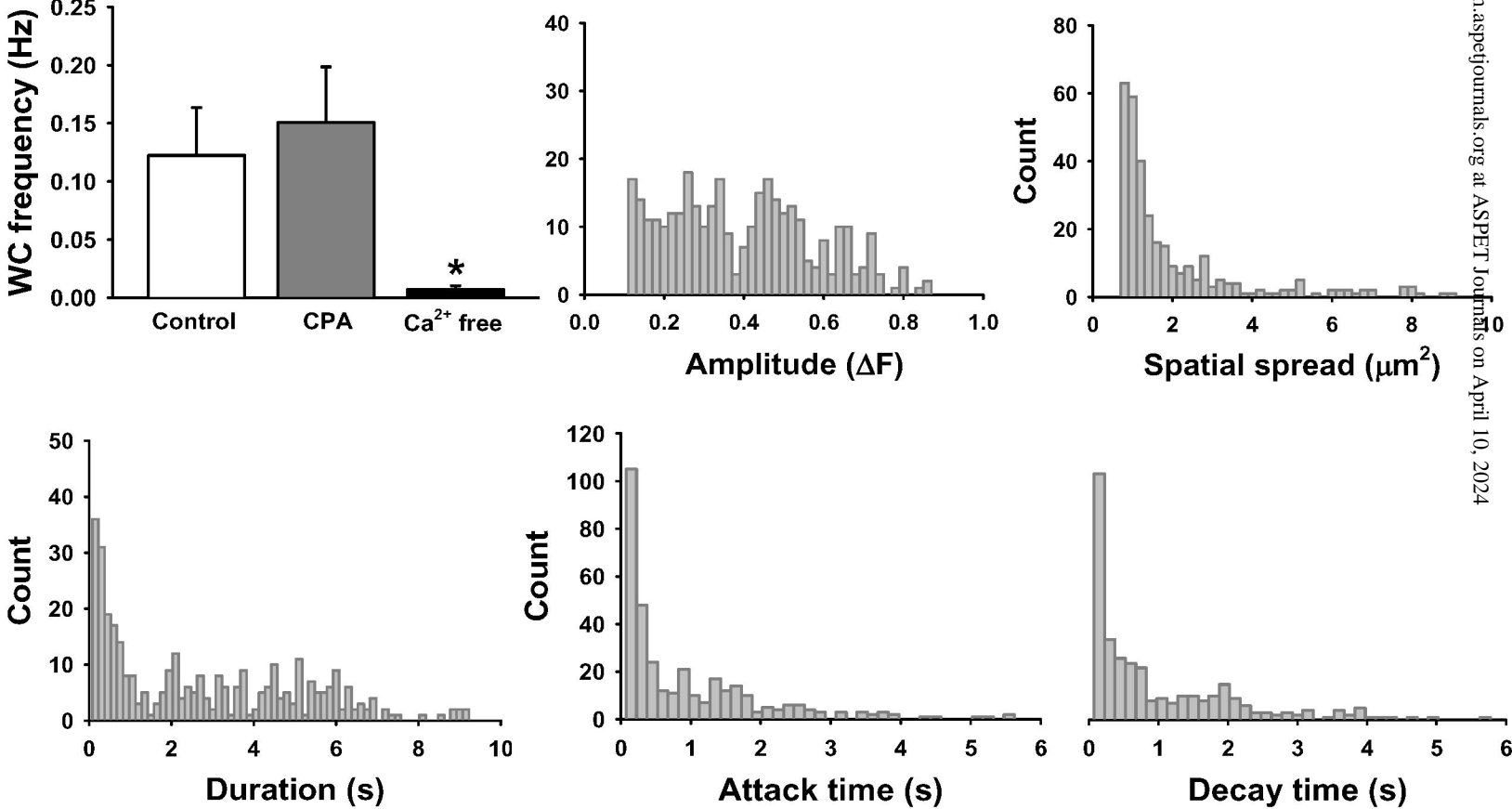


Figure 2

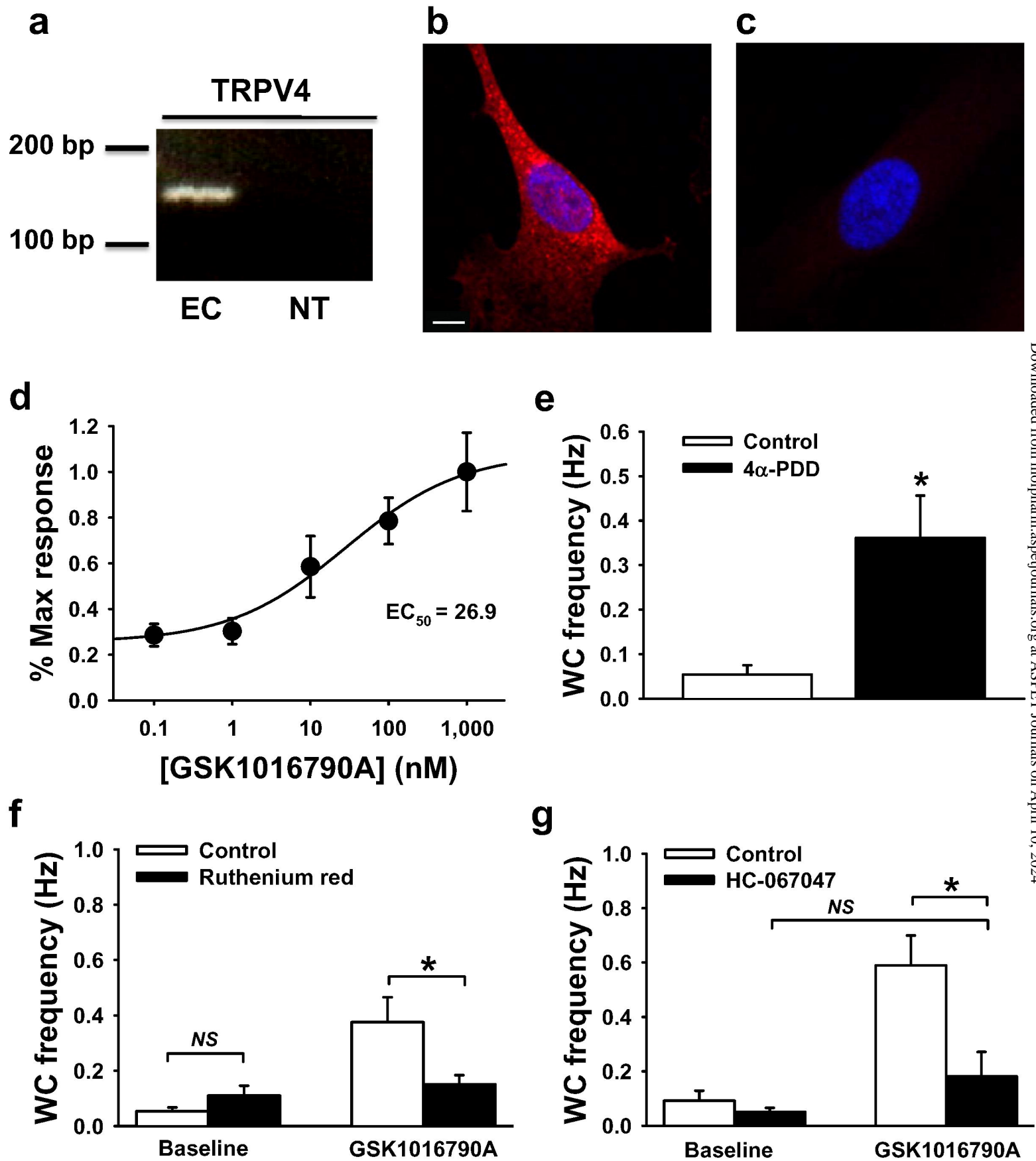
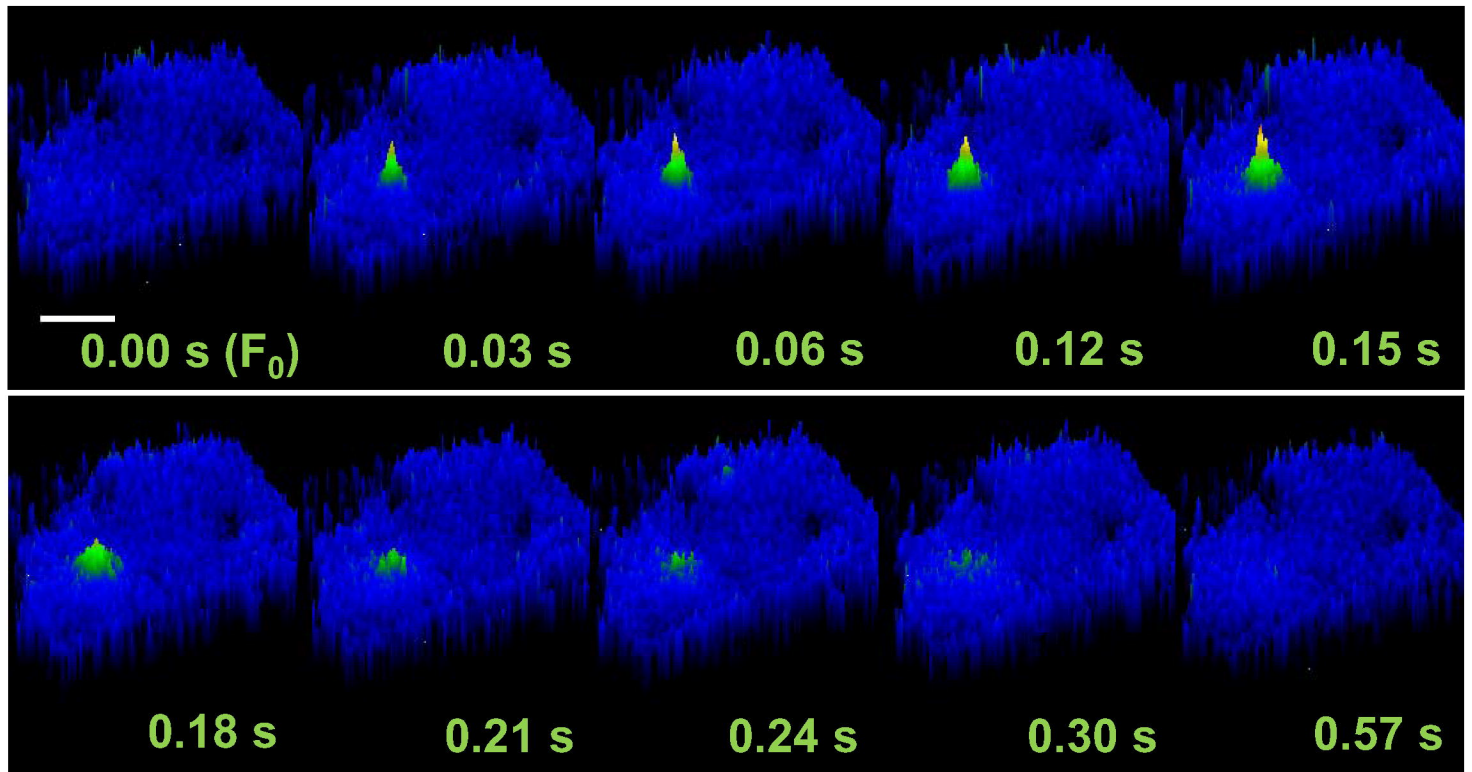
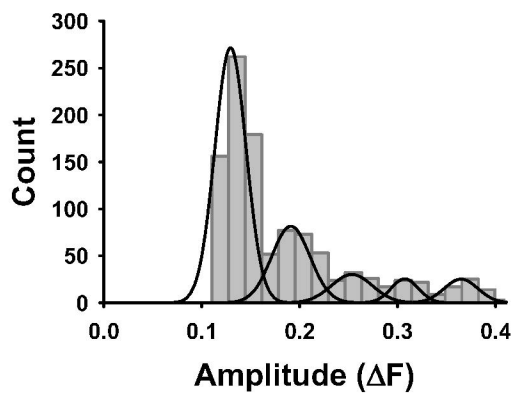


Figure 3

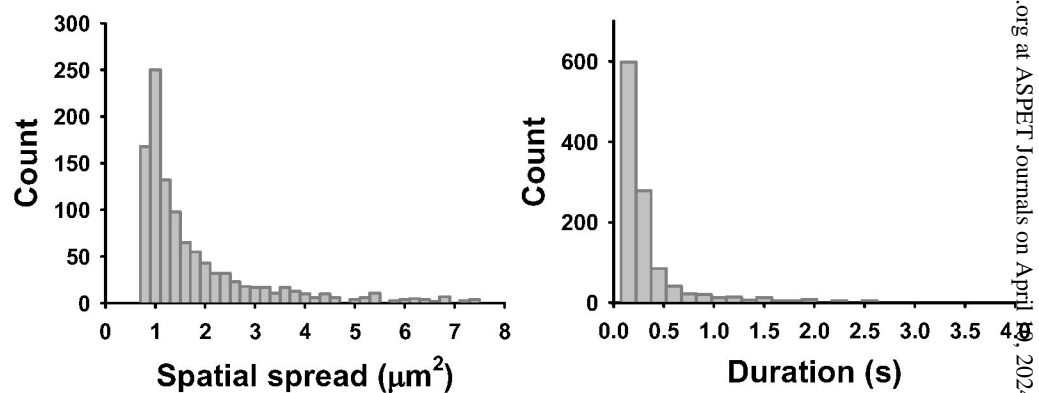
a



b



d



c

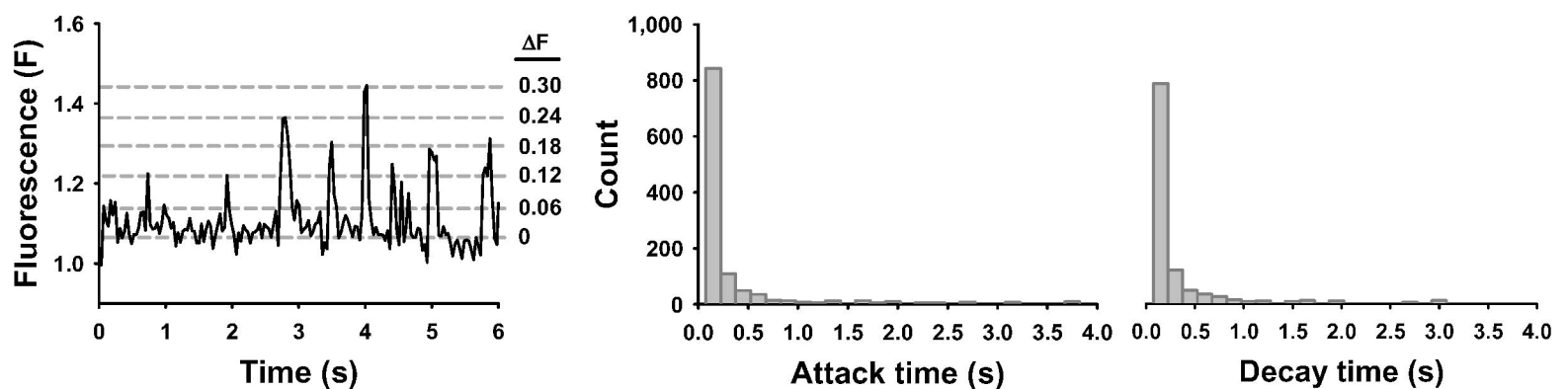
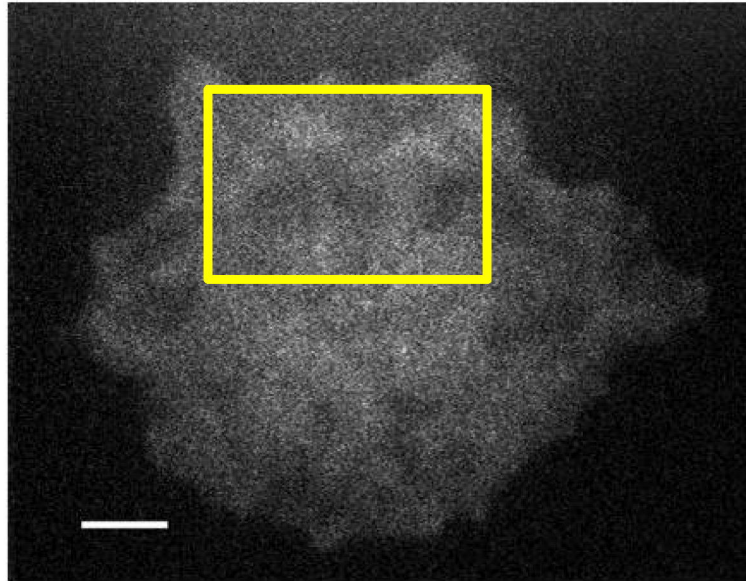


Figure 4

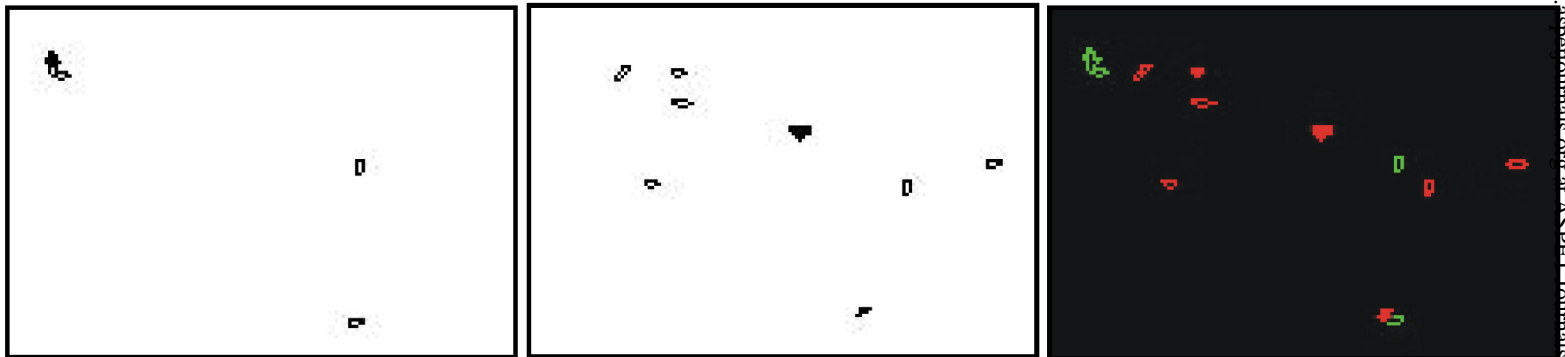
a



Before

After

Merged



b

